2010 IEEE International Conference on Robotics and Automation
Anchorage Convention District
May 3-8, 2010, Anchorage, Alaska, USA

UAV Altitude and Attitude Stabilisation using a Coaxial Stereo Vision System

Richard J. D. Moore, Saul Thurrowgood, Daniel Bland, Dean Soccol & Mandyam V. Srinivasan

Abstract— **This study describes a novel, vision-based system for guidance of UAVs. The system uses two coaxially aligned cameras, each associated with a specially-shaped reflective surface, to obtain stereo information on the height above ground and the distances to potential obstacles. The camera-mirror system has the advantage that it remaps the world onto a cylindrical co-ordinate system that simplifies and speeds up range computations, and defines a collision-free cylinder through which the aircraft can pass without encountering obstacles. We describe an approach, using this vision system, in which the attitude and altitude of an aircraft can be controlled directly, making the system particularly suited to terrain following, obstacle avoidance, and landing. The autonomous guidance of an aircraft performing a terrain following task using the system is demonstrated in field tests.**

I. INTRODUCTION

Unmanned aerial vehicles (UAVs) are increasingly replacing manned systems in situations which are either too dangerous, too remote, or too difficult for a manned aircraft to access. Modern UAVs are capable of accurately controlling their position and orientation in space using systems such as GPS and AHRS (Attitude Heading Reference System). However, they are unable to perform crucial guidance tasks such as obstacle avoidance, low-altitude terrain or gorge following, or landing in an uncontrolled environment using these systems only. For such tasks, the aircraft must be able to continuously monitor its surroundings. The use of active sensors, such as laser range finders or radar has been considered, however such systems can be bulky, expensive, and stealth-compromising. Therefore, there is considerable interest in the design of guidance systems for UAVs that use passive sensing, such as vision.

Over the last two decades, a significant amount of research has shown that biological visual systems can inspire novel, vision-based solutions to some of the challenges of autonomous aircraft guidance (e.g. [1], [2]). A recent trend in biologically inspired vision systems has been to exploit optic flow information for collision avoidance, terrain following, gorge following, and landing [1], [3]–[7]. However, systems that rely on optic flow for extracting range information need to discount components of optic flow that are induced by rotations of the aircraft, and use only those components of optic flow that are generated by the translational component of motion. The reason is that it is only the translational components of optic flow that provide information on the range to objects in the environment. Furthermore, altitude cannot be controlled in a precise manner using measurements of optic flow only, as optic flow also depends upon the aircraft's groundspeed.

This work was supported partly by US Army Research Office MURI ARMY-W911NF041076, Technical Monitor Dr Tom Doligalksi, US ONR Award N00014-04-1-0334, ARC Centre of Excellence Grant CE0561903, and a Queensland Smart State Premier's Fellowship.

Authors are associated with the Queensland Brain Institute & School of Information Technology and Electrical Engineering, University of Queensland, St Lucia, QLD 4072, Australia and ARC Centre of Excellence in Vision Science, Australia. Correspondence via r.moore1@uq.edu.au

Fig. 1. Implementation of the stereo vision system shown mounted on the test aircraft. The aircraft is a Super Frontier Senior-46 (wingspan 2040mm), modified so that the engine and propeller assembly is mounted above the wing.

In this study, we describe a stereo vision system in which the aircraft's altitude may be directly computed and controlled, irrespective of the attitude or groundspeed of the aircraft, and independently of its rotations about the roll, pitch, and yaw axes. Wide-angle stereo systems have previously been designed for aircraft [8]–[10], but they have rarely been tailored to the specific needs of aircraft guidance, such as terrain and gorge following, obstacle detection, and landing. Here we describe a stereo vision system that is specifically designed to serve these requirements.

We also describe a closed-loop control system that has been developed to allow the autonomous control of our test aircraft (Fig. 1) and we present results from recent flight tests that demonstrate the ability of our onboard system to control a UAV fully autonomously, whilst following terrain in an uncontrolled, outdoor environment. Finally, we discuss the ability of our vision system to detect and avoid obstacles autonomously.

A. Vision system concept

The concept of the stereo vision system is best described by considering two coaxially aligned camera-mirror assemblies, as illustrated in Fig. 2. Each camera views the environment through a specially shaped mirror. The derivation of the profile of this mirror is given in [11], and is not repeated here. The mirror is designed to ensure that equally spaced points

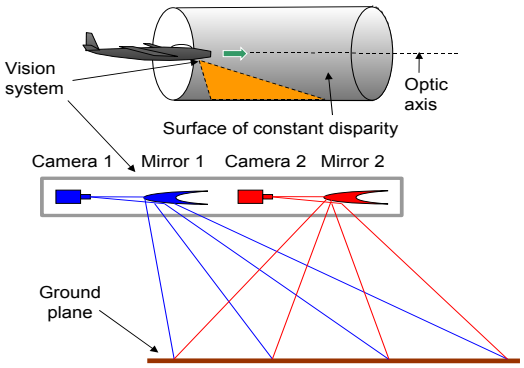

Fig. 2. Schematic illustration of the conceptual stereo vision system, surface of constant disparity, and collision-free cylinder.

on the ground, on a line parallel to the camera's optical axis, are imaged to points that are equally spaced in the camera's image plane.

As a result of this special geometric remapping, the pixel disparity, D_{pixel}, produced by a point imaged in both cameras is inversely proportional to the radial distance, d_{radial}, of that point from the optical axis of the system. The relationship is given by

$$D_{pixel} = \frac{d_{baseline} \times h_{img}}{r} \times \frac{1}{d_{radial}}, \qquad (1)$$

where $d_{baseline}$ is the stereo baseline, h_{img} is the vertical resolution of the remapped images and r, the forward viewing factor, is the ratio of the total forward viewing distance to the height of the aircraft. The first term in (1) is simply a constant which depends on the system configuration. The system parameters and their values used in this study are listed in Table I.

It follows from (1) that the maximum disparity measured by this system, in a given stereo pair, defines the radius of a cylinder of free space surrounding the optical axis through which the aircraft can fly without encountering any obstacles. Hence, this system is well suited to providing information for visual guidance in the context of tasks such as terrain and gorge following, obstacle detection, and landing.

TABLE I
SYSTEM PARAMETERS

Stereo baseline ($d_{baseline}$)	200mm
Remap image cols / rows (h_{img})	128px / 384px
Vertical FoV	0° to 68.2° from vertical
Horizontal FoV	−100° to 100° from vertical
Forward viewing factor (r)	2.5
Detectable disparity (D_{pixel})	0px to 15px
Operational altitude (d_{radial})	2.0m ∼ 40m+

II. STEREO VISION SYSTEM

A. Design

The present implementation of the stereo vision system is an evolution of the system described in [12], and is shown mounted on the test aircraft in Fig. 1. In both systems, the function of the specially shaped mirrors is simulated using software lookup tables. This reduces the physical bulk and cost of the vision system and avoids aberrations due to imperfections in the mirror surface. We have used high resolution video cameras (PGR Grasshopper 20S4M) equipped with wide-angle fish-eye lenses (Sunex DSL215), providing good spatial resolution within a larger field of view.

The two camera assemblies are rigidly mounted in a coaxial stereo configuration to minimise measurement errors resulting from relative motion between the two assemblies during flight. Additionally, we have utilised lightweight miniature lenses to reduce their vibration-induced motion relative to the camera sensors, which presented a problem in the previous system.

Each camera assembly has been calibrated using the generic camera model described in [13] to account for any idiosyncrasies. Additionally, any rotational misalignment between the two cameras is accounted for by applying a corrective rotational transformation to one of the camera models. A non-linear optimisation algorithm was used to determine the appropriate corrective rotation matrix by minimising the pixel difference between a stereo pair of images.

All image processing and higher order functions are performed by the onboard computer (Digital-Logic MSM945 which incorporates an Intel Core2 Duo 1.5Ghz processor). Flight commands are continuously sent to the aircraft's control surfaces through an interface which allows a ground-based human pilot to select between computer controlled autonomous flight and radio controlled manual flight.

B. Operation

Vision based strategies for controlling the altitude of UAVs have been described previously [1], [4], [7], [14]–[16]. However, previous studies have typically relied upon regulating the ventral, longitudinal optic flow observed from the aircraft, and therefore show severe limitations. Firstly, for stable and accurate altitude control, the rotational component of optic flow generated by a change in aircraft pitch must be subtracted from the measured optic flow. This either requires a very large field of view, such that the rotational motion of the aircraft can be distinguished from the translational motion, or an additional apparatus for explicit measurement of the pitch rate, such as a gyroscope.

Secondly, the range perceived from a downward facing camera or optic flow sensor is not only dependent upon altitude and velocity, but also the aircraft's attitude. This is particularly relevant to fixed-wing aircraft in which relatively high roll and pitch angles are required to perform rapid manoeuvres. A method for overcoming these shortcomings is given in [17], however the technique proposed there is too limited to be implemented in practice as it fails to include the roll of the aircraft.

Finally, as with all optic flow-based approaches, to compute an accurate estimate of range, the groundspeed of the

aircraft must be decoupled from the optic flow measurement. In practice this requires additional sensors, such as a high-precision GPS or a pitot tube. Moreover, in the case of the latter, the variable measured is actually windspeed, which would lead to incorrect range estimates in all but the case of low altitude flight in still air.

In this study, we describe a stereo vision system in which the aircraft's altitude can be directly computed and controlled, irrespective of the attitude or groundspeed of the aircraft, and independently of its rotations about the roll, pitch, and yaw axes. We assume that the ground directly beneath and in front of the aircraft (corresponding to the visible FoV, see Table I) can be modelled as a plane. The aircraft's attitude and altitude can then be accurately estimated relative to the ground plane. We have shown in [12] that this is a feasible method for estimating the altitude and attitude of a UAV in an unknown, outdoor environment.

C. Flight control

Range information is extracted from the remapped images by computing the image disparity between the stereo pairs. The algorithm used to compute the disparity is based on the sum of absolute differences (SAD) between images and is described in more detail in [12]. The radial distance from the optical axis to each observed point is computed by rearranging (1). Using the camera calibration results, the 3D location of each point relative to the nodal point of the vision system can also be calculated. Therefore, the visible environment can be reconstructed in three dimensions from the disparity map by reprojecting each point. It was demonstrated in [12] that a simple 3D environment could be accurately reconstructed with a maximum reprojection error of approximately 5% using this system.

In [12] we modelled the ground as a planar surface, computed its disparity profile and used an iterative, non-linear optimisation procedure to fit this profile, in disparity space, to the measured disparity profile of the ground. Here, in contrast, we reproject the disparities according to the method described above, and fit the ground plane to the reprojected points in 3D space. While this procedure does not sample data points uniformly in the plane, it leads to a single-step, non-iterative optimisation that offers the advantage of low computational overheads and reliable real-time operation, which is important in closed-loop control. This approach allows typically ~ 4000 disparity points to be reprojected and the parameters of the plane of best fit to be computed in approximately $1 \sim 2$ms – an improvement of two orders of magnitude over the previous method.

During flight, the vision system and onboard computer provide continuous estimates of the aircraft's altitude and attitude relative to the ground plane. For autonomous flight the onboard computer must also generate the appropriate control commands and communicate them to the aircraft.

In this study we use cascaded PID feedback control loops to generate flight controls whilst minimising the error between the visually estimated altitude and attitude and the respective setpoints. The closed-loop control system is depicted in Fig. 3. Roll and pitch are controlled independently and so full autonomous control of the aircraft is achieved using two feedback control subsystems. Additionally, within each control subsystem, multiple control layers are cascaded to improve the stability of the system.

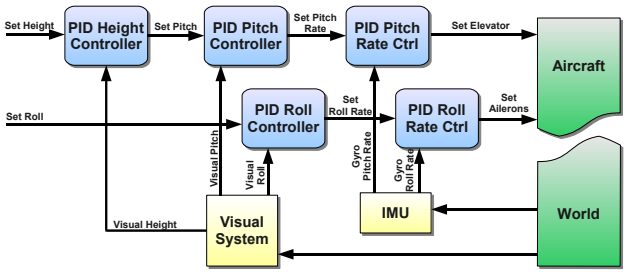

Fig. 3. Block diagram illustrating the closed-loop control scheme.

The control subsystem for stabilising the roll of the aircraft comprises two cascaded PID controllers. The higher level controller measures the error in the roll angle of the aircraft and delivers an appropriate roll rate command to the lower level controller, which implements the desired roll rate. The pitch control subsystem functions identically to the roll subsystem, although it includes an additional, cascaded PID controller to incorporate altitude stabilisation. Shown in Fig. 3, aircraft altitude is regulated by the highest level PID controller which feeds the remainder of the pitch control subsystem.

Measurements of the absolute attitude and altitude of the aircraft are made by the stereo vision system and are used to drive all other elements of the closed-loop control system. Low level control feedback for the roll rate and pitch rate is provided by an onboard inertial measurement unit (MicroStrain 3DM-GX2 IMU). By utilising multiple control layers, the aircraft can be simultaneously driven towards a particular altitude, pitch angle, and pitch rate. This allows finer, more robust closed-loop control and reduces the need for accurately calibrated integral and derivative gains in the PID controllers.

III. FLIGHT TESTING

A. Autonomous terrain following

The system parameters used in the closed-loop flight test are shown in Table I. The vision system has a flight ceiling of $40\text{m} - 50\text{m}$ for obtaining accurate measurements of the aircraft's attitude and height above ground. At this altitude the disparity produced by the ground is < 1px and is below the system noise floor. Therefore, the system was programmed to hold an altitude of 10m above ground level (AGL) during autonomous terrain following. Additionally, the system was programmed to stabilise the aircraft's roll angle with respect to the ground plane.

The closed-loop performance of the vision system was evaluated by piloting the test aircraft in a rough racetrack pattern. During each circuit the aircraft was piloted to attain

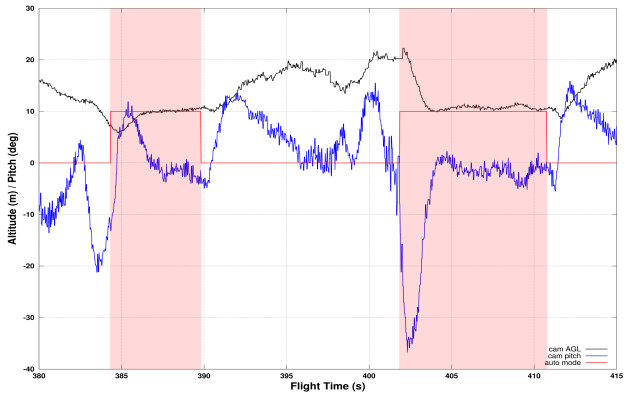

Fig. 4. The visually estimated height (black/solid) and pitch angle (blue/dashed) of the aircraft during a 35s segment of flight. Also shown is a scaled binary trace (red/shaded) that indicates the periods of autonomous control, during which the aircraft was programmed to hold an altitude of 10m AGL.

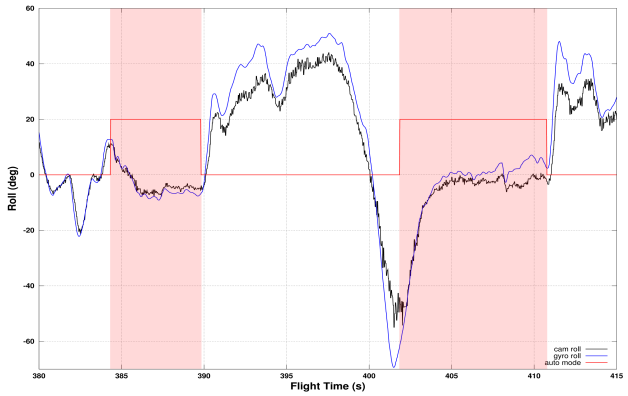

Fig. 5. The visually estimated roll angle (black/solid) of the aircraft during a 35s segment of flight. For comparison, the roll angle reported by the onboard inertial unit is shown (blue/dashed). Also shown is a scaled binary trace (red/shaded) that indicates the periods of autonomous control, during which the aircraft was programmed to hold a roll angle of 0° with respect to the ground plane.

an abnormal altitude and attitude, and then automatic control was engaged for a period of approximately $5\text{s} - 10\text{s}$ to test how well the automatic control was able to restore the set altitude (10m AGL) and roll (0°). This procedure was repeated 18 times during a test flight lasting approximately eight minutes. For each autonomous pass, the aircraft was able to right itself and stabilise its altitude according to the programmed setpoints.

A typical segment of flight during which the aircraft made two autonomous passes has been analysed. Video footage of the aircraft during this segment of flight is shown in the attached video, alongside footage from the front camera onboard the aircraft. Figs. 4 & 5 show the altitude and attitude of the aircraft during the flight segment, as estimated by the stereo vision system.

It can be seen from Fig. 4 that on both passes, once automatic control was engaged, the aircraft was able to attain and hold the desired altitude within approximately 2s – climbing from 6m AGL during the first autonomous pass and descending from approximately 22m AGL during the second.

From Fig. 5 it can be seen that during the second autonomous pass the aircraft was also able to quickly stabilise its attitude despite a severe initial roll angle more than -50° from the horizontal. During the first pass, however, the aircraft overcorrected for the initial error in roll angle and wasn't able to properly stabilise the aircraft, leveling out at approximately -5°. The cause of this error was attributed to improperly balanced gains in the lowest level PID controllers.

Despite this shortcoming the vision system performed well, as is attested by the close correlation between the visually estimated roll angle and that reported by the IMU onboard the aircraft during the test flight. Temporary deviations between the estimated roll and pitch angles and their reported values are to be expected, however, due to the inherent difference between the measurements performed by the stereo vision system, which measures attitude with respect to the local orientation of the ground plane, and the IMU, which measures attitude with respect to gravity.

To obtain a quantitative measure of the robustness and accuracy of the system, the behaviour of the aircraft during each of the 18 autonomous passes was analysed. The visually estimated altitude of the aircraft throughout the flight test is displayed in Fig. 6. It can be seen that in every autonomous pass the aircraft was able to reduce the absolute error between its initial altitude and the setpoint (10m AGL). In most cases, in fact, the aircraft was able to very quickly approach 10m AGL and effectively stabilise its altitude, despite initial altitudes varying between 5m and 25m AGL.

The autonomous performance of the system was measured by considering two metrics. Firstly, the time taken for the aircraft to reach $10\text{m} \pm 1\text{m}$ AGL from the initial altitude was calculated for each of the autonomous passes. This metric gives an idea of the response time of the system. Secondly, the accuracy of the system whilst following terrain was estimated by calculating the average altitude of the aircraft during each autonomous segment, after the aircraft first passed within one metre of the altitude setpoint. This metric incorporates the average steady state error of the system as well as any overshoot or oscillation, but discounts the initial response phase.

From the data, the average response time of the system was calculated as $1.45\text{s} \pm 1.3\text{s}$, where the error bounds represent 2σ from the 18 closed-loop trials. The relatively high variance of the average response time is due to the large range of initial altitudes. Using the second metric defined above, the average unsigned altitude error was calculated as $6.4 \times 10^{-1}\text{m}$ from approximately 92s of discontinuous autonomous terrain following. These performance metrics both indicate that the closed-loop system is able to quickly respond to sharp adjustments in altitude and also that the system is able to accurately hold a set altitude.

Unfortunately, the altitude estimated by the stereo vision system throughout the test flight was unable to be directly corroborated by an independent measurement of the ground

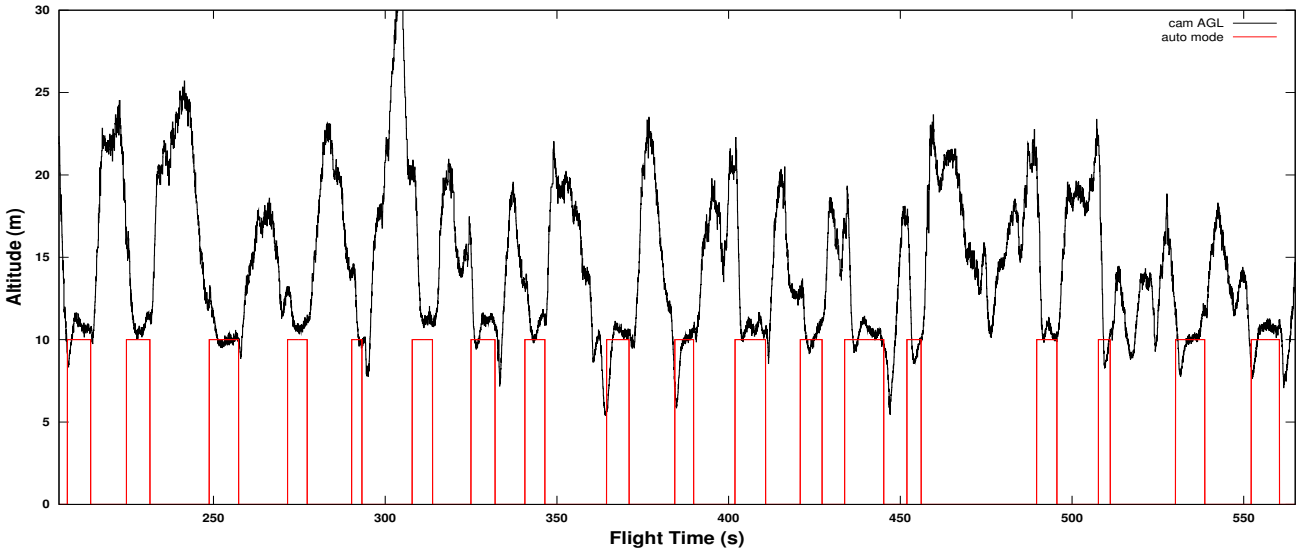

Fig. 6. The visually estimated altitude (black/solid) of the aircraft during the flight test. Also shown is a scaled binary trace (red/dashed) that indicates the periods of autonomous control, during which the aircraft was programmed to hold an altitude of 10m AGL.

truth. The ultrasonic range finder, incorporated into the system for this specific purpose, was unable to provide satisfactory ground truth measurements of the aircraft's altitude at the height above ground at which the test flight was conducted. On the other hand, the ground plane fitted to the reprojected range data is known to provide accurate estimates of the aircraft's attitude, as is demonstrated by the data presented in [12] and Fig. 5. Additionally, it is known that the average range error is less than 5% at low altitudes [12]. Therefore, it can be inferred that the visually estimated altitude is legitimate, particularly at altitudes below 20m where the disparity produced by the ground is approximately twice the system noise floor.

B. Object avoidance

The cylindrical remapping afforded by the vision system provides a simple, yet elegant method by which objects encroaching on the aircraft's trajectory might be identified and avoided. The radial distance from the flight path to objects in the environment can be computed directly from the disparity map. Therefore, a simple control loop can be implemented in which the aircraft is repelled from objects penetrating the notional flight cylinder required by the aircraft for collision-free flight.

Although no such specific object avoidance algorithm has been implemented in the current study, the terrain following algorithm described here is inherently able to guide an aircraft away from obstacles. This stems from the least squares fitting of the ground plane to the reprojected range data. When approaching an obstacle, the visible environment may no longer be represented simply as a plane. However, the plane of best fit will pass through reprojected points corresponding to the ground as well as to the obstacle, causing the aircraft to veer away from the obstacle when correcting for the estimated error in attitude.

It can be seen from Fig. 5 that during the second autonomous pass the roll angle of the aircraft as reported by the IMU deviates from the visually estimated roll angle. The remapped image from the front camera at approximately 410s is displayed in Fig. 7a alongside the corresponding disparity map. It can clearly be seen from Fig. 7b that the tree in the lower left of the remapped image is significantly closer to the optical axis, and hence the flight path, than the ground behind it. Therefore, when an ideal ground plane is fitted to the 3D points reprojected from this disparity data, the plane will pass through both the ground and the tree. Thus the visual estimate of the aircraft's roll angle will be negatively greater than the roll angle of the aircraft estimated from the ground alone. Accordingly, the aircraft will roll to the right to correct the error and hence avoid the tree.

The predicted behaviour of the aircraft in this circumstance would result in the roll angle reported by the IMU increasing positively whilst the roll angle estimated by the stereo vision system remains driven towards zero by the closed-loop control system. This is in fact what is observed from approximately 407s onwards in Fig. 5, where the aircraft approaches a large tree. The magnitude of the response of the system to the obstacle in this case was small, however, because the aircraft was not in danger of colliding with the tree at any stage. Future work will involve further investigation into the ability of the stereo vision system to provide guidance for avoiding obstacles.

C. Vision system performance

The onboard computer and vision system are capable of capturing stereo images, performing the remapping and pre-processing, computing stereo disparities and reprojecting the points, fitting the ground plane, and recording data at $>$ 30Hz. However, during the closed-loop flight test the system was operated at 25Hz to reduce the load on the

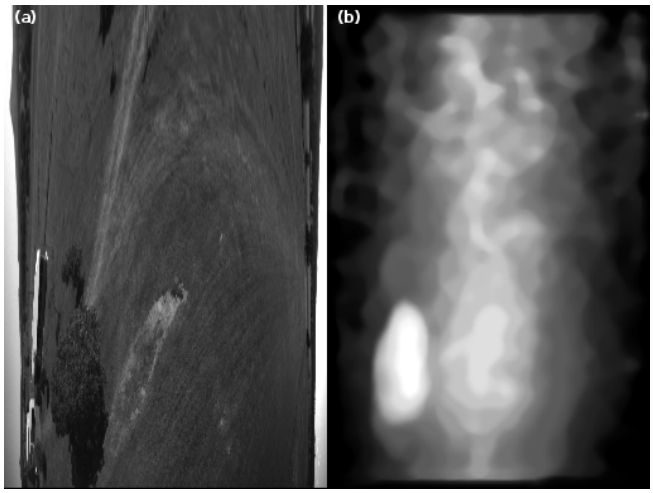

Fig. 7. (a) Remapped image taken from the front camera onboard the aircraft during the closed-loop flight test and (b) the corresponding disparity map. The magnitude of the disparity is inversely proportional to radial distance from the optical axis, in accordance with (1).

onboard computer. Additionally, prior to fitting the ground plane, the disparity maps were downsized to $64\text{px} \times 96\text{px}$, to limit the maximum number of reprojected points used when applying the fit. Images were captured over an IEEE 1394b interface at a resolution of $1072\text{px} \times 1072\text{px}$. Stereo image pairs were synchronised to within $125\mu\text{s}$. Full resolution raw images were recorded onboard at 8.33Hz to facilitate offline analysis of the flight data, however all data presented within this report was computed at 25Hz for real-time, closed-loop control of the aircraft. Other parameters are as listed in Table I.

IV. CONCLUSIONS & FURTHER WORK

This study has described the design and implementation of a vision system which simplifies the computation of range from stereo in the context of aircraft guidance. Two coaxially aligned video cameras are used in conjunction with wide-angle lenses to capture stereo images of the environment, and a special geometric remapping is employed to simplify the computation of range. The maximum disparity, as measured by this system, defines a collision-free space through which the aircraft can fly unobstructed. This system is therefore especially suited to providing information for visual guidance in the context of tasks such as terrain and gorge following, obstacle detection and avoidance, and take-off and landing.

Prior testing has proven that this system is capable of accurately measuring and reproducing the three dimensional structure of simple environments, both indoors and outdoors [12]. In the present study we have taken the next step by demonstrating that the vision system is capable of controlling the attitude of an aircraft in real-time, as well as enabling it to perform terrain following autonomously. We have demonstrated the ability of the vision system to react quickly and effectively to oncoming terrain.

No specific object avoidance algorithm has been implemented in this study. However, the characteristics of our stereo vision system afford a simple yet elegant method by which nearby obstacles may be detected and guidance provided to the aircraft such that they may be avoided. As a next step, it is planned to adapt the system to provide autonomous visual guidance for an aircraft performing tasks related to obstacle detection and avoidance, take-off and landing.

ACKNOWLEDGMENT

Sincere thanks to Mr. David Brennan, who owns and maintains the airstrip at which the flight testing was done.

REFERENCES

[1] M. V. Srinivasan, S. W. Zhang, J. S. Chahl, G. Stange, and M. Garratt, "An overview of insect inspired guidance for application in ground and airborne platforms," *Proc. Inst. Mech. Engnrs. Part G*, vol. 218, pp. 375–388, 2004.

[2] N. Franceschini, "Visual guidance based on optic flow: A biorobotic approach," *Journal of Physiology*, vol. 98, pp. 281–292, 2004.

[3] J. S. Chahl and M. V. Srinivasan, "Panoramic vision system for imaging, ranging and navigation in three dimensions," in *Proc. Field and Service Robotics Conference*, Pittsburgh, Aug. 1999, pp. 127–132.

[4] G. L. Barrows, J. S. Chahl, and M. V. Srinivasan, "Biologically inspired visual sensing and flight control," *The Aeronautical Journal*, vol. 107, no. 1069, pp. 159–168, 2003.

[5] F. Ruffier and N. Franceschini, "Optic flow regulation: the key to aircraft automatic guidance," *Robotics and Autonomous Systems*, vol. 50, pp. 177–194, 2005.

[6] J.-C. Zufferey and D. Floreano, "Fly-inspired visual steering of an ultralight indoor aircraft," *IEEE Trans. Robot.*, vol. 22, pp. 137–146, 2006.

[7] A. Beyeler, J.-C. Zufferey, and D. Floreano, "optipilot: Control of take-off and landing using optic flow," in *Proc. 2009 European Micro Air Vehicle Conference and Competition (EMAV'09)*, 2009.

[8] C. L. Tisse, O. Frank, and H. Durrant-Whyte, "Hemispherical depth perception for slow-flyers using coaxially aligned fisheye cameras," in *Proc. International Symposium on Flying Insects and Robots*, Ascona, Switzerland, Aug. 2007, p. 123.

[9] S. Thurrowgood, W. Stuerzl, D. Soccol, and M. V. Srinivasan, "A panoramic stereo imaging system for aircraft guidance," in *Proc. Ninth Australasian Conference on Robotics and Automation (ACRA'07)*, Brisbane, Australia, Dec. 2007.

[10] J. M. Roberts, P. I. Corke, and G. Buskey, "Low-cost flight control system for a small autonomous helicopter," in *Proc. IEEE International Conference on Robotics and Automation (ICRA'03)*, Taipei, Taiwan, Sep. 2003.

[11] M. V. Srinivasan, S. Thurrowgood, and D. Soccol, "An optical system for guidance of terrain following in UAV's," in *Proc. IEEE International Conference on Advanced Video and Signal Based Surveillance (AVSS'06)*, Sydney, Australia, 2006, pp. 51–56.

[12] R. J. D. Moore, S. Thurrowgood, D. Bland, D. Soccol, and M. V. Srinivasan, "A stereo vision system for UAV guidance," in *Proc. IEEE International Conference on Intelligent Robots and Systems (IROS'09)*, St Louis, MO, Oct. 2009.

[13] J. Kannala and S. S. Brandt, "A generic camera model and calibration method for conventional, wide-angle, and fish-eye lenses," *IEEE Trans. Pattern Anal. Mach. Intell.*, vol. 28, no. 8, pp. 1335–1340, 2006.

[14] W. E. Green, P. Y. Oh, K. Sevcik, and G. Barrows, "Autonomous landing for indoor flying robots using optic flow," in *Proc. ASME International Mechanical Engineering Congress*, Washington, D.C., Nov. 2003.

[15] M. A. Garratt and J. S. Chahl, "Vision-based terrain following for an unmanned rotorcraft," *Journal of Field Robotics*, vol. 25, pp. 284–301, 2008.

[16] J.-C. Zufferey, A. Beyeler, and D. Floreano, "Near-obstacle flight with small UAVs," in *Proc. International Symposium on Unmanned Aerial Vehicles (UAV'08)*, Orlando, FL, Jun. 2008.

[17] A. Beyeler, C. Mattiussi, J.-C. Zufferey, and D. Floreano, "Vision-based altitude and pitch estimation for ultra-light indoor aircraft," in *Proc. IEEE International Conference on Robotics and Automation (ICRA'06)*, 2006, pp. 2836–2841.